

Detachment of an electron from hydrogen, chlorine, or titanium ions colliding with argon, sodium, or magnesium

I. T. Serenkov, R. N. Il'in, and V. I. Sakharov

A. F. Ioffe Physicotechnical Institute, Academy of Sciences of the USSR, Leningrad

(Submitted 27 July 1984)

Zh. Eksp. Teor. Fiz. **88**, 417–425 (February 1985)

The electron detachment cross section σ_{10}^- has been measured for Cl^- and Ti^- with velocities in the range 0.3×10^8 – 10^8 cm/s in collisions with Na, Mg, or Ar atoms. The role of potential and dynamic mechanisms in the detachment process is discussed. It is shown that the latter predominates in the case of electronegative quasimolecules and that the impulse model can then be used to estimate σ_{10}^- . It is shown that the anisotropy of electron scattering must be taken into account in the impulse model of the detachment process.

Electron detachment from negative ions colliding with atoms or molecules is one of the topics in the physics of atomic collisions in which there has been continuing interest in recent years. This interest has been due to two factors, namely, the physics and technology of problems such as the development of injectors of fast hydrogen atoms for thermonuclear reactors, and the fact that this process is an example of the interaction of a single energy term with the continuous spectrum (without the intervention of an intermediate interaction with a region of high density of Rydberg states), and may well turn out to be a convenient testing ground for methods in collision theory. The nature of the detachment process depends on the relative velocity of the colliding particles. Thus, the energy of the system of colliding particles $A^- + B$ may exceed the energy of the neutral quasimolecule $A + B$, and the electron may undergo a transition from a discrete state to the continuum with an energy loss that can be as small as convenient. This particular mechanism is characteristic for low collision velocities, and will be referred to as the potential mechanism. The dynamic mechanism becomes increasingly important with increasing relative velocity and is characterized by the fact that the transition of the electron to the continuum is due to the transfer of a considerable amount of momentum and energy (comparable with its binding energy) to the electron. Theoretical models for collision velocities v that are much lower than the orbital velocity w of an outer electron are based on the consideration of the quasimolecule consisting of the colliding particles. The potential mechanism can be described in terms of the complex potential (the procedure for this is given, for example, in Ref. 1). The zero-range method proposed by Demkov² and developed by Devdariani³ takes into account, besides the potential mechanism, certain dynamic effects.⁴ Recent publications^{4,5} take into account different dynamic effects, particularly transitions associated with the rotation of the internuclear axis, within the framework of the quasimolecular mechanism.

Perturbation-theory methods, for example, the Born method,⁶ can be used at high velocities $v \gg w$. Lopantseva and Firsov⁷ have derived an interesting result for fast collisions. They have shown that the cross section for electron detachment from alkali-metal negative ions colliding with inert-gas

atoms is close to the elastic cross section for the scattering of a free electron traveling with a velocity equal to the velocity of the ion in the same target. Bates and Walker^{8,9} have used similar considerations in the semiclassical impulse approximation, and have treated the detachment of an electron with binding energy ϵ as the scattering of an electron by the target, accompanied by the transfer to it of energy $\Delta E \gg \epsilon$. The target was assumed to be a rigid object of cross section equal to the total cross section for the scattering of a free electron by the target particle under consideration. Calculations performed within the framework of this approach for H^- ions colliding with inert-gas atoms and atmospheric molecules were found to be in satisfactory agreement with experiment for $v \gg w$. All the above models were used to examine the detachment of an electron from the negative ion H^- . There are very few calculations relating to more complicated ions, and those that are available are concerned with velocities $v < w$. They employ different quasimolecular models.

The region in which the collision velocity is close to the orbital velocity of the outer electron usually corresponds to the maximum cross section for restructuring of this shell, and is therefore interesting for a number of applications. On the other hand, it is the most difficult problem for theoretical analysis. It is therefore useful to examine experimentally the process of electron detachment from different negative ions at these velocities. By using ions with different binding energy ϵ , it is possible to establish the role of this parameter in the collision mechanism. In addition to targets with high ionization potentials I , it is useful to employ alkali and alkaline-earth metals which have low I and high polarizability, and differ from one another by the fact that only the former can exist as stable negative ions. Moreover, it has been shown¹⁰ that the cross section of weakly-bound electrons from such targets for the detachment is much lower than the cross section for the scattering of a free electron with the corresponding velocity. The first step in a study of the electron detachment process in the case of negative ions at low velocities can be the experimental determination of the total electron-detachment cross section and, hence, the identification of the most representative targets for this type of investigation.

In view of the foregoing, the aim of our research was to investigate electron detachment by measuring the total cross

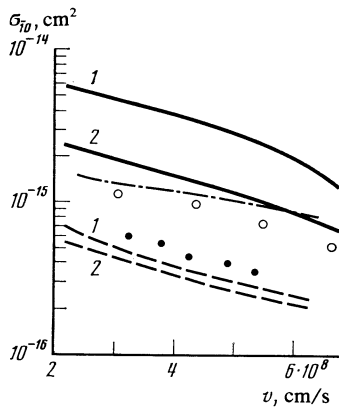


FIG. 1. Electron detachment cross section σ_{10}^- of the H^- ion as a function of its velocity for the following targets: (1) sodium atoms: \circ —our experiment, dash-dot curve taken from Ref. 11, solid curves 1 and 2— isotropic and anisotropic electron scattering models, respectively; (2) H_2 molecules: \bullet —our experiment, dashed curves 1 and 2— isotropic and anisotropic electron scattering models, respectively.

section σ_{10}^- for this process for collision velocities in the range $0.3 \leq v \leq 10^8$ cm/s (20–200 keV for intermediate-mass ions). The projectiles were Cl^- ($\epsilon = 3.62$ eV) and Ti^- ($\epsilon = 0.08$ eV), and the targets were sodium, magnesium, and argon. To check the validity of the model describing the scattering of a weakly-bound electron at high velocities ($2 \leq v \leq 6 \times 10^8$ cm/s), we have also measured the cross section σ_{10}^- for the pair (H^- , Na).

1. EXPERIMENTAL METHOD

The experimental setup was in the form of a double mass spectrometer. Ions were produced by a high-frequency ion source into which titanium tetrachloride vapor was introduced. Negative ions were formed by charge transfer between the corresponding positive ions in the exit channel of the ion source. The negative-ion beam produced in this way was focused and then accelerated to 25–250 keV. After magnetic analysis and collimation, the beam was allowed to enter the target chamber filled with the required gas or vapor. The metal-vapor pressure was measured by determining

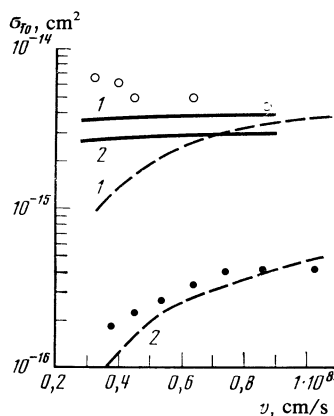


FIG. 2. Electron detachment cross section of Cl^- and Ti^- ions colliding with Na atoms: \bullet — Cl^- , experiment, dashed curves—calculated; \circ — Ti^- , experiment, solid curves—calculated (1, 2— isotropic and anisotropic electron scattering, respectively).

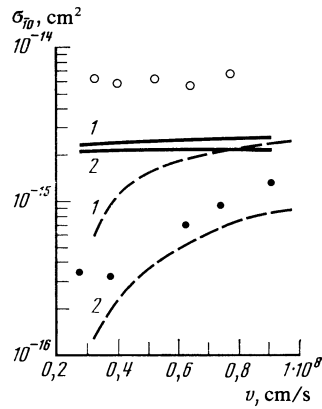


FIG. 3. Electron detachment cross section of Cl^- and Ti^- ions colliding with Mg atoms. See Fig. 2 for notation.

the temperature of the heated chamber. The beam leaving the target chamber was separated by a magnetic field into components of different charge. Negative ions, atoms, and singly-charged positive ions were recorded at the same time by counting the individual particles with an efficiency in excess of 90%. The detectors could be used to record beams with a divergence of up to 1° . The cross section for electron detachment from a fast negative ion, σ_{10}^- , was determined from the ratio of the flux of the atoms to the total flux of fast particles, and was plotted as a function of the pressure in the target chamber. The cross section determined in this way was the sum of the cross section for the removal of an electron to the continuum and the cross section for charge transfer with the formation of the negative target ion. However, for the targets that we have examined, the formation of stable negative ions is possible only in sodium and, as will be shown below, the charge-transfer cross section is much smaller than the cross section for the removal of the electron to the continuum in our range of collision velocity. This enables us to assume that the measured cross section is, in fact, the cross section for the detachment of a single electron.

RESULTS AND DISCUSSION

Figures 1–4 show our measured cross section σ_{10}^- as functions of collision velocity. The cross section $\sigma_{10}^-(v)$ was measured for H^- ions colliding with sodium atoms and hydrogen molecules at high collision velocities ($3 \leq v \leq 6.5 \times 10^8$ cm/s) in order to verify the validity of the impulse model developed by Bates and Walker⁹ for different targets. The same figures show, for comparison, the cross section $\sigma_{10}^-(v)$ measured in Ref. 11 for the pair (H^- , Na). Figures 2–4 compare these cross sections for Cl^- and Ti^- ions colliding with sodium, magnesium, and argon atoms. Figure 4 shows, for comparison, the velocity dependence of the cross section measured in Ref. 12. Comparison of the measured cross section $\sigma_{10}^-(v)$ for Cl^- and Ti^- shows that the two are close to one another in the case of argon atoms, whilst the cross sections for Ti^- on sodium and magnesium atoms are slowly-varying functions of velocity, and are much higher than the cross sections for Cl^- .

Figures 2–4 also show the function $\sigma_{10}^-(v)$ calculated for

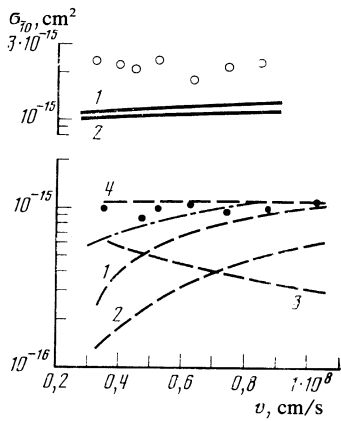


FIG. 4. Electron detachment cross section of Cl^- and Ti^- ions colliding with argon atoms. See Fig. 2 for notation. In addition: curve 3 refers to Cl^- and was calculated by CPM, whereas curve 4 was calculated from NSM; the dot-dash curve shows the experimental data from Ref. 12.

different theoretical models. These data can be used to examine the relative importance of potential and dynamic mechanisms in electron detachment, and the validity of the different models. We have assumed that the velocity dependence $\sigma_{10}(v)$ obtained in the impulse approximation to the scattering of a weakly-bound electron⁹ reflects, at least qualitatively, the contribution of the dynamic mechanism, provided the following factors are taken into account. The contribution of the potential σ_{10} cannot exceed πR_0^2 , where R_0 is the point at which the original $(A+B)^-$ term crosses the continuous-spectrum limit of $(A+B)$. This contribution can be determined more precisely by using the complex potential method (CPM). The data necessary for these calculations are given below for specific pairs of colliding particles.

(H^-, Na) and (H^-, H_2) pairs

It is clear from Fig. 1 that the cross sections σ_{10} for H^- , Na, calculated from the formula given in Ref. 9 (solid curve 1), exceed the experimental values by several times. On the other hand, the corresponding cross sections obtained for (H^-, H_2) are in good agreement with experimental results. The reason for this discrepancy cannot be the excitation of the colliding particles. The H^- ion has excited states lying in the continuum, but they are short-lived as compared with electron detachment. Possible excitation of the sodium atom was taken into account in the calculation by using the total cross section (including both excitation and ionization of the target) instead of the elastic cross section for electron scattering. All the same, the cross sections σ_{10} obtained from the elastic and the total cross sections are not very different.

Satisfactory agreement between calculations and experiment was achieved by taking into account the anisotropy in electron scattering (IES) by the sodium atom (Fig. 1, solid curve 2). Actually, the differential electron-scattering section $d\sigma_e(\theta)/d\Omega$ of sodium and other alkali and alkaline-earth metals assumes high values at low scattering angles for which the momentum and energy received by the electron are insufficient for its detachment. On the other hand, the authors of Ref. 9 assumed in their derivation of the working formula that the electrons were scattered isotropically (IES)

by the target, and used the total scattering cross section. The procedure that we have used to take into account the scattering anisotropy is described in the Appendix.

The anisotropy in the scattering of electrons by H_2 molecules and by the molecules of atmospheric gases and inert-gas atoms is small. This is the reason why, as can be seen from Fig. 1, the calculations performed for (H^-, H_2) with and without the anisotropy corrections produce very similar results.

Figures 2, 3, and 4 show the cross section σ_{10} for Cl^- and Ti^- , calculated for isotropic electron scattering (curves 1) and for anisotropic electron scattering (curves 2). For the Cl^- ion, which has a high binding energy ϵ , the two models yield very different cross sections even in the case of argon, whereas for Ti^- , which has a low ϵ , a substantial difference between the two models occurs only in the case of sodium atoms. The total cross sections for electron scattering by Na, Mg, and Ar atoms and the H_2 molecules were taken from Refs. 13–16, the differential cross sections were taken from Refs. 17–20, and the binding energies of Cl^- and Ti^- were taken from Refs. 21 and 22, respectively. The method used to calculate the orbital electron velocity w is given in the Appendix.

(Cl^-, Na) and (Cl^-, Mg) pairs

The cross sections $\sigma_{10}(v)$ calculated from the impulse models are similar to the experimental results, but the isotropic scattering model yields values that are much too high, whereas the anisotropic scattering model is in good agreement with experiment. This leads us to the conclusion that the dynamic mechanism is the dominant effect in the velocity range that we have considered. The fact that the potential mechanism is relatively unimportant for (Cl^-, Na) at collision velocities $v \leq 10^7$ cm/s was demonstrated in Ref. 23 and was explained by the absence of a crossing between the (Na, Cl) and (Na, Cl^-) potential curves. The charge-transfer cross section is also apparently small in comparison with σ_{10} . The energy lost in this process is 3 eV and, as shown in Ref. 24, the charge-transfer cross section becomes small in comparison with the electron-detachment cross section even for the $\text{H}^- + \text{Na} \rightarrow \text{H} + \text{Na}^-$ process for which the energy loss is only 0.2 eV for $v > 0.4 \times 10^8$ cm/s. Moreover, charge transfer is impeded by the presence of the $[\text{Cl}^-, \text{Na}(3p)]$ term lying between the (Cl^-, Na) and (Cl, Na^-) terms.

An analogous situation obtains for (Cl^-, Mg) . The cross section $\sigma_{10}(v)$ calculated from the anisotropic electron scattering model is in satisfactory agreement with experiment for $v < 0.4 \times 10^8$ cm/s, i.e., for the velocity range in which the dynamic mechanism is again predominant. It is shown in Ref. 25 that the stable ion MgCl^- exists, so that the crossing of the (Mg, Cl^-) and (Mg, Cl) terms, if it occurs, should take place for internuclear distances definitely smaller than the equilibrium value of 2.2×10^{-8} cm.

The above examples show that, although the validity of the impulse model is, strictly speaking, problematic for velocities $v < 10^{-8}$ cm/s, in our case the model gives the correct value and the velocity dependence for the electron detachment cross section due to the dynamic mechanism. The

introduction of an additional factor representing the independent interaction between each outer electron and the target, as was done in Ref. 9, does not seem to us to be justified, at any rate for the velocities under consideration. On the other hand, it is possible that a correction for the dimensions of the outer shell has to be introduced in this velocity range. This is indicated by the results reported in Ref. 26.

The (Cl, Ar) pair

Figure 4 shows $\sigma_{10}^-(v)$ calculated from the impulse (isotropic and anisotropic electron scattering) and quasimolecular (CPM and NSM) models, and also the corresponding experimental data. The data on the shape of the (Ar, Cl⁻) and (Ar, Cl) energy terms near the crossing point that are necessary for calculations are taken from Refs. 27 and 28. It is clear from Fig. 4 that neither the potential (CPM) nor the dynamic (isotropic and anisotropic) mechanism is capable of reproducing the measured $\sigma_{10}^-(v)$. The NSM model is based on the potential mechanism, but includes certain dynamic effects. It yields $\sigma_{10}^-(v)$ that is in good agreement with experiment, both qualitatively and quantitatively. All this suggests that both mechanisms are effective in our velocity range for this particular pair of colliding particles, and both provide appreciable contributions to the electron detachment probability. It is interesting to note that the sum of cross sections σ_{10}^- calculated from the potential (CPM) and dynamic (anisotropic electron scattering) models is close to the measured value. These data provide us with a clear idea about the relative contributions of the two mechanisms that we have considered and, in addition, show that the anisotropic electron scattering model is better than the isotropic model. The authors of Ref. 12, which appeared simultaneously with our preliminary publication,²⁹ suggest that the relatively high cross sections σ_{10}^- obtained at high velocities are due to transitions that occur above the continuous-spectrum limit when the original (Cl⁻, Ar) term approaches excited terms such as (Cl*⁻, Ar) and (Cl, Ar⁻). In our view, this explanation is less satisfactory than that relying on the contribution of the dynamic mechanism that increases with velocity, since the cross section σ_{10}^- in this particular velocity range is approximately equal to πR_0^2 and there are no additional transitions above the continuous-spectrum limit, i.e., the cross section cannot increase beyond this value for internuclear separations $R < R_0$.

(Ti⁻, Na), (Ti⁻, Mg), and (Ti⁻, Ar) pairs

Comparison of experimental data obtained for Ti⁻ ions with calculations based on anisotropic and isotropic models shows that, for all Mg and Ar targets and all the velocities that we have considered, and also for sodium in the case of $v > 0.4 \times 10^8$ cm/s, the measured and calculated cross sections $\sigma_{10}^-(v)$ lie on similar curves. The cross sections obtained from the anisotropic and isotropic models are similar to each other, but are lower than the measured values by factors of about 2–3. The complexity of the system in terms, especially for Ti⁻ interacting with metal atoms, and the absence of reliable calculations for these systems, prevented us from carrying out a rigorous calculation based on the CPM

model. The estimated upper limit $\sigma_{10}^- < \pi R_0^2$, determined by calculating the internuclear separation corresponding to the crossing of the (Ti⁻, Na) term and the continuous-spectrum limit, using the zero³⁰ and finite-range³¹ models, gave 6×10^{-15} and 13×10^{-15} cm² but, in accordance with the CPM model, these values should decrease with increasing velocity. Removal of the 4s electron, leaving behind the Ti atom in the 3d²4s configuration, may contribute to the detachment process. This process requires relatively little expenditure of energy at infinity ($\Delta E = 0.9$ eV), and this may decrease as a result of the promotion of the 4s σ -orbital of Ti⁻. It is important to note that the charge-transfer process $\text{Ti}^- + \text{Na} \rightarrow \text{Ti} + \text{Na}^-$ is possible for this pair, and this may be responsible for the reduction in $\sigma_{10}^-(v)$ with increasing velocity for $v < 0.4 \times 10^8$ cm/s. Since the cross section is in better agreement with the potential mechanism, and its dependence on the velocity is in better agreement with the dynamic mechanism, we cannot choose between the two.

To summarize, we have measured the electron detachment from cross sections for Cl⁻ and Ti⁻ ions colliding with sodium, magnesium, and argon atoms at ion velocities in the range $0.3 \leq v < 10^8$ cm/s, i.e., velocities somewhat lower than the orbital velocities of the weakly bound electron in the negative ions employed in these experiments. Comparison of the measured cross sections with calculations based on models reflecting different detachment mechanisms shows that both the potential and the dynamic mechanisms provide considerable contributions to the process, but the latter becomes predominant for $v > 10^8$ cm/s.

Comparison of the functions $\sigma_{10}^-(v)$ for different projectiles and targets has shown that the properties of these functions in the velocity range that we have investigated are determined by the possibility of a bound negative molecular ion consisting of the two colliding particles. For pairs that can combine in this way, the cross section σ_{10}^- is relatively small and increases with increasing velocity, whereas the detachment process is almost wholly determined by the dynamic mechanism. In the opposite case, the cross sections are large and much less dependent on velocity, and the detachment process is due to the combined effect of the two mechanisms. The transition from the situation in which the potential mechanism is predominant to that in which the dynamic mechanism is the more important is best illustrated by the (Cl⁻, Ar) pair. Although this suggests the quasimolecular nature of collisions in those cases where detachment is exclusively determined by the dynamic mechanism, the function $\sigma_{10}^-(v)$ can be satisfactorily predicted by the impulse model developed for higher velocities by Bates and Walker.

We have also shown that the impulse model of electron scattering, used to calculate the detachment cross section for a weakly bound electron at arbitrary collision velocity, must be corrected for anisotropy, at least for targets with strong electron scattering anisotropy and high polarizability, e.g., alkali and alkaline-earth metals. For negative ions, the contribution of this effect increases with increasing binding energy of the outer electron.

The authors are indebted to E. A. Solov'ev for useful discussions and M. É. Raïkh for assistance in calculations.

APPENDIX

It follows from the analysis given in Ref. 8 that the detachment cross section for an electron moving with velocity v can be written in the form

$$\sigma_{i0}(v) = \int_{w=0}^{\infty} \int_{\varphi=0}^{\pi} \int_{\theta=0}^{\pi} \Phi \sigma_e(u, \theta) f(w) \sin \varphi \sin \theta dw d\varphi d\theta, \quad (1)$$

where $f(w)$ is the orbital velocity distribution of outer electrons in the negative ion, $\mathbf{u} = \mathbf{v} + \mathbf{w}$, $\sigma_e(u, \theta)$ is the differential cross section for the scattering of a free electron incident on the target with velocity u , φ is the angle between the vectors \mathbf{v} and \mathbf{w} , and Φ is proportional to the electron detachment probability, i.e., to the probability that the electron will receive additional kinetic energy exceeding the binding energy ε (in atomic system of units):

$$\begin{aligned} \Phi &= 0 \text{ for } \mu \geq 1, \\ \Phi &= \arccos \mu \text{ for } -1 \leq \mu \leq 1, \quad \Phi = \pi \text{ for } \mu \leq -1, \end{aligned} \quad (2)$$

where

$$\mu = [\varepsilon - v(w \cos \varphi + v)(1 - \cos \theta)] / vw \sin \theta \sin \varphi.$$

To simplify our calculations, we have assumed that

$$f(w) = \delta(w - w_0), \quad (3)$$

where w_0 is the mean orbital velocity of a weakly bound electron. Equation (1) then assumes the form

$$\sigma_{i0}(v) = \int_{\varphi=0}^{\pi} \int_{\theta=0}^{\pi} \Phi \sigma_e(u, \theta) \sin \theta \sin \varphi d\theta d\varphi. \quad (4)$$

Transformations analogous to those made in Ref. 8 for an electron scattered isotropically (isotropic electron scattering model) then yield

$$\sigma_{i0}(v) = \frac{1}{4vw_0} \int_{u_0}^{v+w_0} u \sigma_e(u) \left[1 + \frac{u}{2v} + \frac{v^2 - w_0^2 - 2\varepsilon}{2vu} \right] du, \quad (5)$$

where

$$\begin{aligned} u_0 &= v - w_0 \text{ for } w_0 \leq v - \varepsilon/2v, \\ u_0 &= (2\varepsilon + w_0^2)^{1/2} - v \text{ for } w_0 \geq v - \varepsilon/2v. \end{aligned}$$

Calculations based on (5) and those based on the formula obtained in Ref. 9 on the assumption that $f(w)$ was the same as the electron velocity distribution in the hydrogen atom, give for the above velocity range results that differ by not more than 30%.

When the assumption of isotropic electron scattering was inadmissible (anisotropic scattering model), the calculations were based on (4). The differential electron scattering cross section in this expression was taken from the literature for velocities closest to the larger of the two velocities v and w_0 .

To take into account the dependence of the differential cross section on velocity u in the determination of $\sigma_{i0}(v)$, the latter was multiplied for each v by the ratio $\sigma_1(v)/\sigma_2(v)$, where $\sigma_1(v)$ and $\sigma_2(v)$ were calculated from (5) and, in the calculation of $\sigma_2(v)$, the cross section $\sigma_e(u)$ in (5) was replaced with the constant quantity σ_3 determined from

$$\sigma_3 = 2\pi \int_0^{\pi} \sigma_e(\max(v, w_0), \theta) \sin \theta d\theta. \quad (6)$$

We have calculated the velocity w_0 by using the Hartree-Fock wave functions with parameters taken from Refs. 32 and 33. For the state described by a wave function of the form $\Psi(r, \theta, \phi) = R(r)Y_{lm}(\theta, \phi)$ with radial function $R(r)$ and orbital angular momentum l , the velocity is

$$w_0 = \int_0^{\infty} w f(w) dw,$$

where

$$f(w) = \frac{2w^2}{\pi} \left[\int_0^{\infty} R(r) j_l(wr) r^2 dr \right]^2 \left[\int_0^{\infty} R^2(r) r^2 dr \right]^{-1}$$

and

$$j_l = (-1)^l \frac{r^l}{w^{l+1}} \left(\frac{d}{r dr} \right)^l \frac{\sin(wr)}{r}.$$

The velocity w_0 , calculated in this way for Cl^- and Ti^- , was 0.726 and 0.934 atomic units, respectively.

- ¹S. K. Lam, J. B. Delos, R. L. Champion, and L. D. Doverspike, Phys. Rev. A **9**, 1828 (1974).
- ²Yu. N. Demkov, Zh. Eksp. Teor. Fiz. **46**, 1126 (1964) [Sov. Phys. JETP **19**, 762 (1964)].
- ³A. Z. Devdariani, Zh. Tekh. Fiz. **43**, 399 (1973) [Sov. Phys. Tech. Phys. **18**, 255 (1973)].
- ⁴J. P. Gauyacq, Comments Atom. Mol. Phys. **10**, 171 (1981).
- ⁵T. S. Wang and J. B. Delos, Phys. Rev. A **29**, 542 (1984).
- ⁶M. R. C. McDowell and G. Peach, Proc. Phys. Soc. London **74**, 463 (1959).
- ⁷G. B. Lopantseva and O. B. Firsov, Zh. Eksp. Teor. Fiz. **50**, 975 (1966) [Sov. Phys. JETP **23**, 648 (1966)].
- ⁸D. R. Bates and J. C. G. Walker, Planet Space Sci. **14**, 1367 (1966).
- ⁹D. R. Bates and J. C. G. Walker, Proc. Phys. Soc. London **90**, 333 (1967).
- ¹⁰V. A. Oparin, R. N. Il'in, and E. S. Solov'ev, Zh. Eksp. Teor. Fiz. **52**, 369 (1967) [Sov. Phys. JETP **25**, 240 (1967)].
- ¹¹C. J. Anderson, R. J. Gurnius, A. M. Howald, and L. W. Anderson, Phys. Rev. A **22**, 822 (1980).
- ¹²B. Hird and F. Rahman, J. Phys. B **16**, 3581 (1983).
- ¹³A. Kasdan, T. M. Miller, and B. Bederson, Phys. Rev. A **8**, 1562 (1973).
- ¹⁴N. I. Romanyuk, O. B. Shpenik, A. I. Zhukov, and I. P. Zapesochnyĭ, Pis'ma Zh. Tekh. Fiz. **6**, 877 (1980) [Sov. Tech. Phys. Lett. **6**, 379 (1980)].
- ¹⁵R. D. Du Bois and M. E. Rudd, J. Phys. B **8**, 1474 (1975).
- ¹⁶S. Trajmar, D. G. Truhlar, and J. K. Rice, J. Chem. Phys. **52**, 4502 (1970).
- ¹⁷S. K. Srivastava and L. Vuškovič, J. Phys. B **13**, 2633 (1980).
- ¹⁸W. Williams and S. Trajmar, J. Phys. B **11**, 2021 (1978).
- ¹⁹J. F. Williams and B. A. Willis, J. Phys. B **8**, 1670 (1975).
- ²⁰B. Van Wingerden, E. Weigold, F. J. de Heer, and K. J. Nygaard, J. Phys. B **10**, 1345 (1977).
- ²¹H. Hotop and W. C. Lineberger, J. Phys. Chem. Reference Data **4**, 539 (1975).
- ²²C. S. Feigerle, R. R. Corderman, S. V. Bobashev, and W. C. Lineberger, J. Chem. Phys. **74**, 1580 (1981).
- ²³C. De Vreugd, R. W. Wijnaendts van Resandt, J. Los, B. T. Smith, and R. L. Champion, Chem. Phys. **42**, 305 (1979).
- ²⁴R. E. Olson, Proc. Second Intern. Symposium on the Production and Neutralization of Negative Hydrogen Ions and Beams, Brookhaven Nat. Lab., 1980, pp. 51-17.
- ²⁵V. M. Dukel'skiĭ, E. Ya. Zandberg, and N. I. Ionov, Zh. Eksp. Teor. Fiz. **20**, 877 (1950).
- ²⁶N. Andersen, T. Andersen, and L. Jepsen, J. Phys. B **17**, 2281 (1984).
- ²⁷R. L. Champion and L. D. Doverspike, Phys. Rev. A **13**, 607 (1976).
- ²⁸R. E. Olson and B. Liu, Phys. Rev. A **17**, 1568 (1979).
- ²⁹I. T. Serenkov, V. I. Sakharov, E. A. Solovjev, and R. N. Il'in, Abstracts

of Contributed Papers of Thirteenth Intern. Conf. on the Physics of Electronic and Atomic Collisions, West Berlin, 1983, p. 404.

³⁰B. M. Smirnov and O. B. Firsov, Zh. Eksp. Teor. Fiz. **47**, 232 (1964) [Sov. Phys. JETP **20**, 156 (1965)].

³¹B. M. Smirnov, Atomnye stolknoveniya i élementarnye protsessy v plazme (Atomic Collisions and Elementary Processes in Plasmas), Ato-

mizdat, Moscow, 1968 p. 223.

³²E. Clementi, A. D. McLean, D. L. Raimondt, and M. Yoshimine, Phys. Rev. A **133**, 1274 (1964).

³³E. Clementi, Phys. Rev. A **135**, 981 (1961).

Translated by S. Chomet